Basic characteristics of a photon counting x-ray detector with a CdTe semiconductor

F. Kaibuki[1], T. Kobayashi[1], K. Ogawa[1], T. Yamakawa[2], T. Nagano[2], D. Hashimoto[2] and H. Nagaoka[2]
[1]Faculty of Science and Engineering, Hosei University, Tokyo, Japan, [2]Telesystems Co., Osaka, Japan

1. INTRODUCTION

The development of a pixelated semiconductor detector with CdTe or CdZnTe, which is available for x-ray imaging, has been pursued by many researchers [1–3]. In the case of x-ray imaging the photon flux is very high, and thus most conventional detectors including ones used for x-ray CT adopt an energy integration of detected photons. However, a detector that enables a photon counting mode can yield the energy information of an individual photon. And this kind of information yields advantages in terms of dose reduction, improvement of the signal to noise ratio of an object, reduction of beam-hardening artifacts and discriminating materials. The requirement of a photon counting detector for x-ray imaging is a high count rate such as 10^6–10^8 counts/sec/mm^2, and a spatial resolution of several ten to hundred micron meters. And we developed a new CdTe semiconductor detector with a dedicated application-specific integration circuits (ASICs) that count each photon with four energy windows[4]. In this paper, we outlined the performance of our newly developed photon counting detector and compared our detector with a conventional energy integration detector in terms of the signal to noise ratio.

2. SPECIFICATIONS OF THE DETECTOR

We developed a detector consisting of 18 CdTe detector modules and ASICs designed in CMOS 0.25 μm technology. Each module consisted of 40 x 40 pixels (pixel size: 0.2 x 0.2 mm^2). We adopted a Schottky contact with Aluminum to improve the energy resolution and reduce the dark current. The side onto which the radiation impinges was covered with a continuous Pt electrode, and the pixel electrode was Al, and Sn–Bi was used for a bump-bonding material to the ASICs. We collected only electrons as a carrier. The bias voltage -500 V was applied to the Pt common electrode on the CdTe crystal with a thickness of 1 mm. Each pixel had an integrating preamp and shaper with adjustable shaping time (500 or 300 nsec). The output of the shaper then went into a bank of four comparators with adjustable thresholds. Each comparator output went to a counter of 10-12 bits.

3. MEASURMENT OF THE PERFORMANCE

We evaluated the performance of the detector in terms of following items. For x-ray tubes, TRIX-150S (Torec, Japan) and L9121 (Hamamatsu Photonics, Japan) were used.

3.1 Count rate performance

We used an x-ray tube L9121 and changed the tube current from 10 μA to 90 μA. The tube voltage was 90 kV (Al filter: 2.5 mm). The data acquisition time was 1 sec. We measured the mean count of the detector module located at the center of the active area with a size of 40 x 640 pixels. The results showed a good linearity between the tube current and the count rate up to a count rate of 0.4 x 10^6 counts/sec/pixel.

3.2 Uniformity

We used an x-ray tube TRIX-150S. We set a tube current of 1.0 mA, and tube voltage of 90 kV(Al filter: 2.5 mm). Data acquisition time was 8 sec. In front of the detector we put a PMMA with a thickness of 25 mm. We detected dead pixels in which photons are abnormally measured beforehand and replaced the count with the average of the neighboring pixels. The uniformity was evaluated numerically with the integral uniformity of the pixel values in the active area. The averaged integral uniformity of the four bins was 1.26 %, and the ratio of defect pixels was 0.5 %.

3.3 Spatial resolution

We used an x-ray tube TRIX-150S. We set a tube current of 1.0 mA, and tube voltage of 90 kV(Al filter: 2.5 mm). And we used a resolution chart 'x-ray test chart (type 7)' (Mitsubishi Chemical Co., Japan), in which there were eight slit patterns (0.5 - 5.0 lp/mm). To avoid Moire´ patterns caused by interference between the slit patterns and the pixel alignment we set this chart with a small tilting angle to the pixel alignment in the detector. The resolution chart was located just in front of the detector. The results showed that the spatial resolution of the detector was 2–2.5 lp/mm, which is the theoretical upper limit of the resolution.

3.4 Energy resolution

We operated this detector in a thermostatic chamber at 25 C. We used the standard sources of Am-241 (photopeak energy: 60 keV) and Co-57 (122 keV). The number of pixels used in this measurement was 1600, and we used one module without the calibration of the gain of each pixel. The measurement of the energy spectra was conducted by changing the threshold level of the ASIC, and measuring the number of photons with only one energy window. The data acquisition time was 1 min. We subtracted the total measured count with the succeeding measured count with the different threshold energy, and obtained the energy spectra of Am-241 and Co-57. The results showed that the energy resolution of the detector was 7.5 % FWHM at 60 keV and 4.4 % FWHM at 122 keV.

3.5 Imaging performance

We conducted experiments with several phantoms using an x-ray tube TRIX-150S. The tube voltage was 60 kV and the tube current was 1 mA (Al filter: 2.5 mm). The data acquisition time was 1 s. The filter used was aluminum with a width of 2.5 mm. Fig.1 shows the image of ICs and transistors. The quality of the image was good.

3.6 Comparison with the energy integration detector

We evaluated our photon counting detector with an energy integration detector that had almost the same specifications of a CdTe crystal except for the data acquisition mode. The compared detector was SCAN300F (Ajat Oy, Finland). The active area of this detector was 6.4 x 151.0 mm^2 (64 x 1510 pixels) with the size of a pixel on the detector 0.1 x 0.1 mm^2. The thickness of the detector was 0.75 mm. We compared the performance of our detector and SCAN300F with a step wedge phantom made of aluminum, in which the thickness of the aluminum increased from 4.5 mm to 31.5 mm in 3 mm increments (nine steps). The x-ray tube (TRIX-150S) with a voltage of 90 kV and tube current of 0.6 mA (Al filter: 2 mm) was used. The data acquisition time was 3 ms for both detectors. For our detector we set four energy thresholds (30, 45, 60 and 75 keV), and acquired four energy binned images (bin0: 30–44 keV, bin1: 45–59 keV, bin2: 60–74 keV, and bin3: 75–90 keV). The performance of the detectors was evaluated as regards the signal to noise ratio in an ROI set at each step position. We defined the signal to noise ratio here as (measured mean count)/(standard deviation in the same ROI). And the theoretical values of the S/N were calculated by (measured mean count)/(square of the mean count). However, the numbers of detected counts differed between two detectors. For example, the number of averaged detected count in the integration detector was 80 with a 0.1 x 0.1 mm^2 pixel in a given area, while that of averaged detected count with the photon counting detector was 10 with a 0.2 x 0.2 mm^2 pixel in the same area. To make a fair comparison we made the size of a pixel to 0.2 x 0.2 mm^2 in the case of the energy integration detector, i.e., we added four pixels and calculated the signal to noise ratio. In that case the calculated signal to noise ratio also differed in each other, so we normalized the signal to noise ratio for each detector. Fig. 2 shows the normalized S/N of the integration type detector and our detector. This graph shows that our detector well agrees to the theoretical S/N, and this means that our detector could perfectly eliminate the electrical noise originated in the circuits. Fig. 3 shows the image of the step wedge phantom at the part where the numeric embossments exist. In this image we added four pixel values and made a 0.2 x 0.2 mm^2 pixel for the energy integration detector. And we normalized the pixel values so as to compare the image with the same display range for a fair comparison.

4 DISCUSSION

In this paper we showed performance of our newly developed detector that was available for measuring photons with four specified energy windows. Our detector shows good linearity between the tube current and output counts up to a count rate of 0.4 x 10^6 counts/sec/pixel (10^7 counts/sec/mm^2). This means we can use this detector under high flux x-rays. As for the energy resolution of the detector, the resultant resolution without any offset calibration was acceptable for the CdTe semiconductor area detector. The uniformity of our detector was quite good for each energy bin and the number of dead pixels was very small with a modification of the guard ring on the surface of each module. And even for these dead pixels we could correct their value by referring to the surrounding pixels. As for the spatial resolution, our detector accomplished almost the theoretical resolution limit of 2-2.5 lp/mm and we could obtain a high quality image in Fig.1. Figs. 2 and 3 show the results of a comparison between our photon counting detector and energy integration detector. Our detector accomplished a reduction of the electrical noise, so that we could achieve theoretical limit in terms of the signal to noise ratio. And this increases the image contrast even though under the count level of 10. The results of these experiments showed that the overall performances of our detector were acceptable for practical application with a photon counting method.

5 CONCLUSION

We showed the performance of our newly developed photon counting detector. Our detector realized a high signal to noise ratio compared with the energy integration type CdTe semiconductor detector.

Fig. 1 Image of ICs and transistors with the energy bin1.

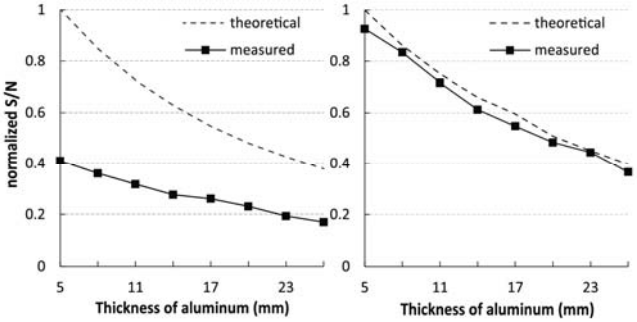

Fig. 2 Signal to noise ratio of the energy integration type detector (left) and our photon counting detector (right).

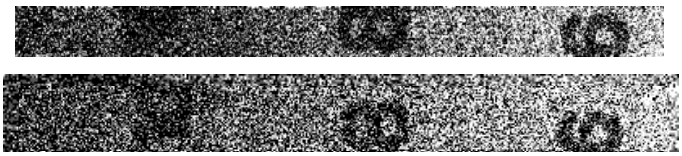

Fig. 3 Images of the step wedge phantom in the step level 10 (thick part) to 6 (thin part). Upper is by the energy integration detector and lower is our photon counting detector.

REFERENCES

1. Meng L.J, Tan J.W, Spartiotis K, Schulman T (2009) Preliminary evaluation of a novel energy-resolved photon-counting gamma ray detector. Nucl Instr Meth Phys Res A 604:548-554
2. Tlustos L (2010) Spectroscopic X-ray imaging with photon counting pixel detectors. Nucl Instr Meth Phys Res A 623:823-828
3. Szeles C, Soldner S et al. (2008) CdZnTe Semiconductor Detectors for Spectroscopic X-ray Imaging. IEEE Trans Nucl Sci, vol. 55, No. 1: 572-582
4. Ogawa K, Kobayashi T, Kaibuki F, et al. (2012) Development of an energy-binned photon-counting detector for X-ray and gamma-ray imaging. Nucl Instr Meth Phys Res A 664:29-37